inorganics

MDPI

Article

A Series of Lanthanide Complexes with Keggin-Type Monolacunary Phosphotungstate: Synthesis and Structural Characterization

Vladimir S. Korenev *, Taisiya S. Sukhikh and Maxim N. Sokolov

Nikolaev Institute of Inorganic Chemistry, Siberian Branch of Russian Academy of Sciences, Lavrentieva St. 3, 630090 Novosibirsk, Russia
* Correspondence: wkorenev@niic.nsc.ru

Abstract: The coordination of rare-earth metal ions (Ln^{3+}) to polyoxometalates (POM) is regarded as a way of modifying and controlling their properties, such as single-molecular magnetism or luminescent behavior. The half-sandwich complexes of Ln^{3+} with monolacunary Keggin POMs (Ln^{3+}/POM = 1:1) are of particular interest, since the Ln^{3+} retains its ability to coordinate extra ligands. Thus, the knowledge of the exact structures of 1:1 Ln/POM complexes is important for the development of reliable synthetic protocols for hybrid complexes. In this work, we isolated three 1:1 Gd^{3+}/POM complexes of the general formula $Cat_4Gd(PW_{11}O_{39})\cdot xH_2O$ (Cat = K^+ or Me_4N^+). Complex $(Me_4N)_2K_2[Gd(H_2O)_2PW_{11}O_{39}]\cdot 5H_2O$ (**1**) is polymeric, revealing a layered structural motif via bridging Gd^{3+} and K^+ ions. Complexes $(Me_4N)_6K_2[Gd(H_2O)_3PW_{11}O_{39}]_2\cdot 20H_2O$ (**2**) and $(Me_4N)_7K[Gd(H_2O)_3PW_{11}O_{39}]_2\cdot 12H_2O$ (**3**) are classified as dimeric; the difference between them consists of the different crystal packing of the polyoxometalates, which is induced by a variation in the cationic composition. Isostructural complexes have also been characterized for praseodymium, europium, terbium and dysprosium. The coordination number of Ln^{3+} (8) persists in all the compounds, while the binding mode of the POM varies, giving rise to different architectures with two or three H_2O co-ligands per Ln^{3+}. However, whatever the particular structure and exact composition, the $\{Ln(PW_{11}O_{39})\}$ moieties are *always* involved in bonding with each other with the formation either of polymeric chains or dimeric units. In water, these aggregates can dissociate with the formation of $[Ln(H_2O)_4PW_{11}O_{39}]^{4-}$. This behavior must be taken into account when choosing L for the design of hybrid {Ln(L)POM} complexes.

Keywords: lanthanide substituted; polyoxotungstate; monovacant Keggin-type

check for updates

Citation: Korenev, V.S.; Sukhikh, T.S.; Sokolov, M.N. A Series of Lanthanide Complexes with Keggin-Type Monolacunary Phosphotungstate: Synthesis and Structural Characterization. *Inorganics* **2023**, *11*, 327. https://doi.org/10.3390/inorganics11080327

Academic Editor: Antonino Gulino

Received: 30 June 2023
Revised: 27 July 2023
Accepted: 27 July 2023
Published: 1 August 2023

1. Introduction

The class of polyoxometalates (POMs) is characterized by great structural diversity with a small number of stable, well-studied structural types [1–3]. Heterometallic derivatives of POMs obtained for a large number of chemical elements with different electronic configurations exhibit various electronic [4,5], magnetic [6–10], catalytic [11–14], optical [15], or other useful properties [16,17]. The wide possibilities of modification determine POM applicability in such areas as biology and medicine, electrochemistry, materials and surface sciences, solar energy conversion, etc. [18–21]. It has been shown that almost all transition and non-transition metals can be included in the vacancy of lacunary Keggin-type POMs, which are the most common [22].

The combination of polyoxometalates with lanthanide (Ln) ions is also interesting from the point of view of unique functional properties, such as, for example, luminescence [23]. One of the principles for the formation of new functional materials is the binding of POM fragments through the Ln ions due to their large coordination numbers, resulting in solid-state oligomers [24,25] and large ring structures [26,27]. POMs can serve as connectors and transfer agents for different monolacunary POMs [28].

A lot of different lanthanide complexes with the monovacant Keggin-type anion, $[PW_{11}O_{39}]^{7-}$, have been well studied to date. These Ln-POMs can be divided into several structurally determined types. First of all, there are the monomeric species containing only one polyoxometalate unit. A series of chromophore-Ln-POMs $[N(CH_3)_4]_3K_2[Ln(C_7H_5O_2)(H_2O)_2(PW_{11}O_{39})]\cdot 11H_2O$ (Ln = Eu, Tb, Tm, Lu) was prepared using $LnCl_3\cdot 6H_2O$ and benzoic acid. Also, with the variation of the molar ratio of Eu:Tb:Tm ions, a series of multicenter-Ln analogues $[N(CH_3)_4]_3K_2[Eu_xTb_yTm_{1-x-y}(C_7H_5O_2)(H_2O)_2(PW_{11}O_{39})]\cdot 11H_2O$ were synthesized [29]. More organic–inorganic hybrid lanthanide-based POMs, $[N(CH_3)_4]_3K_2[Ln(C_7H_5O_2)(H_2O)_2(PW_{11}O_{39})]\cdot 11H_2O$, were synthesized using the same conditions with $HoCl_3\cdot 6H_2O$ [30], $SmCl_3\cdot 6H_2O$ [31] and $TbCl_3\cdot 6H2O$ [32]. In all these cases, the dilacunary $[P_2W_{19}O_{69}(H_2O)]^{14-}$ was used as a source of the resulting Keggin anion. The interaction of phthalocyanine complexes of lanthanides, [Ln(Pc)(OAc)] (Ln = Y, Dy, Tb), with the $[PW_{11}O_{39}]^{7-}$ anion in a 1:1:1 mixture of CH_3CN:MeOH:CH_2Cl_2 also yielded a row of monomeric complexes $(N(nBu)_4)_4H_2[Ln(Pc)(PW_{11}O_{39})]$ [33].

The second group includes dimeric complexes connected through the organic bridging ligands. In 2009, the series of polyoxoanions, $[\{(PW_{11}O_{39})Ln(H_2O)(CH_3COO)\}_2]^{10-}$ (Ln = Sm, Eu, Gd, Tb, Ho, Er), constructed from two monolanthanide substituted $\{PW_{11}\text{-}Ln\}$ units bridged by two acetato ligands, was published [34]. The row was continued with Dy-, Y- and Lu-containing analogues in 2012 [35]. In 2013, $Na_2[Cu(en)_2(H_2O)]_4[\{(PW_{11}O_{39})Sm(H_2O)(CH_3COO)\}_2]\cdot 10H_2O$ [36] and $K_2[Cu(en)_2(H_2O)]_4[\{(PW_{11}O_{39})Tb(H_2O)(CH_3COO)\}_2]\cdot 15H_2O$ [37] had the same hybrid acetate-bridging dimeric structures modified by $[Cu(en)_2(H_2O)]^{2+}$ (en = 1,2-ethylenediamine) fragments. In 2012, four new oxalate-bridging lanthanide-substituted phosphotungstates $\{[(PW_{11}O_{39})Ln(H_2O)]_2(C_2O_4)\}^{10-}$ (Ln = Y, Dy, Ho, Er) were synthesized by the reaction of a Keggin-type anion with Ln cations and oxalate ligands in aqueous solution [38]. The double-tartaric bridged phosphotungstates formulated as $[N(CH_3)_4]_6K_3H_7[Ln(C_4H_2O_6)(PW_{11}O_{39})]_2\cdot 27H_2O$ (Ln = Dy, Er, Yb [39] and Tm [40]) have been obtained using the dilacunary $[P_2W_{19}O_{69}(H_2O)]^{14-}$ as a precursor. In 2012, the hydrothermal conditions were successfully used to prepare the three-dimensional architectures $[Ln(HL)(L)(H_2O)_6\{Ln(H_2L)_{0.5}(PW_{11}O_{39}H)Ln(H_2O)_4\}]_2\cdot nH_2O$ (Ln = La, Ce, Pr; H_2L = 2,5-pyridinedicarboxylic acid) based on lanthanide-substituted POM units [41].

The largest number of examples to date refers to the third type—dimeric complexes in which POM fragments are linked directly through lanthanide cations. In 1971, Peacock and Weakley isolated several dimeric compounds, formulated as $K_{11}[Ce^{III}(PW_{11}O_{39})_2]\cdot 24H_2O$, $K_{10}[Ce^{III}(PW_{11}O_{39})_2]\cdot 25H_2O$, $K_{11}[Pr(PW_{11}O_{39})_2]\cdot 22H_2O$ $K_{11}[Nd(PW_{11}O_{39})_2]\cdot 26H_2O$ [42]. In 2004, the structure of $Cs_{11}Eu(PW_{11}O_{39})_2]\cdot 28H_2O$ was published [43]. The Ce^{IV} sandwiched between two lacunary Keggin-type $[PW_{11}O_{39}]^{7-}$ anions resulted in a lanthanide polyoxometalate $(NH_4)_2[N(CH_3)_4]_6Na_2[Ce(PW_{11}O_{39})_2]\cdot 14H_2O$ [44]. The central $\{Ce^{IV}O_8\}$ polyhedron reveals the square-antiprismatic geometry. The analogues dimeric compound was further prepared for praseodymium, $[(CH_3)_4NH]_4Na_3[Pr(PW_{11}O_{39})_2]\cdot 12H_2O$ [45]. The two isostructural anions, $[Ce^{III}(PW_{11}O_{39})_2]^{11-}$ and $[Ce^{IV}(PW_{11}O_{39})_2]^{10-}$, were isolated as dimethylammonium salts with the same square-antiprismatic coordination of the central $\{Ce^{III/IV}O_8\}$ polyhedron [46]. Interestingly that for similar complexes, $[N(CH_3)_4]_{10}H[La(PW_{11}O_{39})_2]\cdot 21H_2O$ and $[N(CH_3)_4]_{10}H[Ce(PW_{11}O_{39})_2]\cdot 19H_2O$, an approximate cubic $\{LnO_8\}$ geometry was found [47]. Potassium- or mixed potassium/caesium salts of $[Ln(PW_{11}O_{39})_2]^{11-}$ dimeric anions were obtained and characterized for ten lanthanids (Ln = Pr, Nd, Eu, Gd, Tb, Dy, Ho, Er, Tm and Yb) [48]. Three phosphors based on polyoxotungstates, $K_3Cs_8[Eu(PW_{11}O_{39})_2]\cdot 11H_2O$, $K_3Cs_8[Sm(PW_{11}O_{39})_2]\cdot 10H_2O$ and $K_5Cs_6[Dy(PW_{11}O_{39})_2]\cdot 15H_2O$, were prepared and characterized [49]. In 2017, a dysprosium-containing phosphotungstate compound, $K_2[N(CH_3)_4]_5H_4[Dy(PW_{11}O_{39})_2]\cdot 21H_2O$, was published [50].

Separately, a series of novel polyoxometalate trimers, $H_3[N(CH_3)_4]_{14}[NaLn(PW_{11}O_{39})_3]\cdot 18H_2O$ (Ln = Nd, Sm, Eu), can be noted. Herein, the dimeric unit $\{Ln(PW_{11}O_{39})_2\}$ and Na-substituted POM monomer $\{NaPW_{11}O_{39}\}$ linked to form an unprecedented linear structure [51].

Organic–inorganic hybrid enantiomeric compounds of $K_{1.3}Na_{3.2}H_{6.5}[L\text{-}Pr(PW_{11}O_{39})_2]\cdot 8.3L\text{-}proline\cdot 21.5H_2O$, $K_{1.3}Na_{3.2}H_{6.5}[D\text{-}Pr(PW_{11}O_{39})_2]\cdot 8.3D\text{-}proline\cdot 17H_2O$, $K_{1.3}Na_{3.2}H_{6.5}[L\text{-}Er(PW_{11}O_{39})_2]\cdot 8.3L\text{-}proline\cdot 22.5H_2O$ [52] and $KNa_3[Hproline]_7[Sm(PW_{11}O_{39})_2]\cdot D\text{-}proline\cdot 18H_2O$ [53] were obtained by using L- and D-proline as chiral auxiliary agents. The series was expanded by the isolation of $[Ln(PW_{11}O_{39})_2]^{11-}$ polyanions (Ln = La, Pr, Nd, Sm, Eu, Gd, Tb, Dy, Er, Tm, Yb and Y) using proline [54].

In 2008, compound $[Cu(en)_2]_2H_8[Gd(PW_{11}O_{39})_2]\cdot(H_2en)_{0.5}\cdot 3H_2O$ prepared under hydrothermal conditions was described [55]. In 2010, more inorganic–organic hybrid Ln-POM compounds with en-copper-complexes, $H_8[Cu(en)_2H_2O]_4[Cu(en)_2]\{[Cu(en)_2][La(PW_{11}O_{39})_2]\}_2\cdot 18H_2O$, $H_6[Na_2(en)_2(H_2O)_5][Cu(en)_2H_2O]_4[Cu(en)_2]\{[Cu(en)_2][Ce(PW_{11}O_{39})_2]\}_2\cdot 16H_2O$, $H_6[Na_2(en)_2(H_2O)_5][Cu(en)_2H_2O]_4[Cu(en)_2]\{[Cu(en)_2][Pr(PW_{11}O_{39})_2]\}_2\cdot 18H_2O$, $H_6[Na_2(en)_2(H_2O)_4][Cu(en)_2H_2O]_4[Cu(en)_2]\{[Cu(en)_2][Nd(PW_{11}O_{39})_2]\}_2\cdot 14H_2O$, $H_6[Na_2(en)_2(H_2O)_5][Cu(en)_2H_2O]_4[Cu(en)_2]\{[Cu(en)_2][Sm(PW_{11}O_{39})_2]\}_2\cdot 20H_2O$ and $H_7[Cu(en)_2]_2[Sm(PW_{11}O_{39})_2]\cdot 10H_2O$, were published [56]. In 2011, complexes $H_{14}[Cu(en)_2]_4[Ce(PW_{11}O_{39})_2]_2\cdot 2en\cdot 21H_2O$, $H_{14}[Cu(en)_2]_4[Pr(PW_{11}O_{39})_2]_2\cdot 11H_2O$ and $H_8[Cu(en)_2H_2O]_4[Cu(en)_2]\{[Cu(en)_2][Pr(PW_{11}O_{39})_2]\}_2\cdot 2en\cdot 12H_2O$ were presented [57]. A series of 3d–4f heterometallic monovacant Keggin phosphotungstate derivatives, $[Cu(dap)(H_2O)_2]_{0.5}[Cu(dap)_2]_4H_2[Pr(PW_{11}O_{39})_2]\cdot 3H_2O$ (dap = 1,2-diaminopropane), $[Cu(en)_2(H_2O)]_2[Cu(en)_2]_{1.5}H_4[Pr(PW_{11}O_{39})_2]\cdot 10H_2O$ [58], $[Cu(en)_2]_2H_6[Ce(PW_{11}O_{39})_2]\cdot 8H_2O$, $[Cu(dap)_2(H_2O)][Cu(dap)_2]_{4.5}[Dy(PW_{11}O_{39})_2]\cdot 4H_2O$ [59], $[Cu(dap)_2]_{5.5}[Y(PW_{11}O_{39})_2]\cdot 4H_2O$ [60], $Cu(dap)_2(H_2O)][Cu(dap)_2]_{4.5}[Sm(PW_{11}O_{39})_2]\cdot 5H_2O$, $[Cu(dap)_2(H_2O)][Cu(dap)_2]_{4.5}[Er(PW_{11}O_{39})_2]\cdot 4H_2O$ [61], $[Cu(dap)_2(H_2O)][Cu(dap)_2]_{4.5}[La(PW_{11}O_{39})_2]\cdot 4H_2O$ [62] and $H[Cu(dap)_2(H_2O)][Cu(dap)_2]_4[Eu(PW_{11}O_{39})_2]\cdot 13H_2O$ [63], was prepared in hydrothermal conditions.

The first 2:2 type monolanthanide substituted POM dimers, $[\{(PW_{11}O_{39}H)Ln(H_2O)_3\}_2]^{6-}$ (Ln = Nd, Gd), have been published in 2009. The binding of the $[PW_{11}O_{39}Ln(H_2O)_3]^{4-}$ anionic fragments in this structure was provided by two Ln-O-W bridges [34]. In 2017, a dysprosium-containing 2:2 type dimer, $Na_2[N(CH_3)_4]_4H_2[\{Dy(PW_{11}O_{39})(H_2O)_3\}_2]\cdot 28H_2O$, was obtained [50].

One more types of compounds include the chains built from Ln-POMs. Complex $Al(H_3O)[Eu(H_2O)_2PW_{11}O_{39}]\cdot 20H_2O$ was obtained in 2004, and in the solid state, it was an infinite one-dimensional zigzag polymer. A Europium atom coordinated to the POM vacant site was served as the linking element and connected to neighboring $\{PW_{11}O_{39}\}$ units via terminal oxygen atoms [43]. In 2011, the same 1-D zigzag chain was found for $[N(CH_3)_4]_4[Ce(H_2O)_2(PW_{11}O_{39})]\cdot 2H_2O$ with linking $[Ce(H_2O)_2]^{3+}$ cations [64]. Another chain-like structure was found for $[N(CH_3)_4]_4[Tb(H_2O)_2(PW_{11}O_{39})]\cdot 2H_2O$. In this case, the Tb^{3+} cation coordinated with the POM unit vacancy was connected to the terminal oxygen of only one adjacent $\{PW_{11}O_{39}\}$ to form a linear chain [65].

Herein, we present a series of 1:1 Ln^{3+}/POM complexes (Ln = Pr, Eu, Gd, Tb, Dy) of the general formula $Cat_4Ln(PW_{11}O_{39})\cdot xH_2O$ (Cat = K^+ or Me_4N^+). In the case of gadolinium compounds, we found three types of structures: complex $(Me_4N)_2K_2[Gd(H_2O)_2PW_{11}O_{39}]\cdot 5H_2O$ (**1Gd**) is polymeric, revealing a layered structural motif, and complexes $(Me_4N)_6K_2[Gd(H_2O)_3PW_{11}O_{39}]_2\cdot 20H_2O$ (**2Gd**) and $(Me_4N)_7K[Gd(H_2O)_3PW_{11}O_{39}]_2\cdot 12H_2O$ (**3Gd**) are classified as dimeric. For the sake of simplicity, we formulate the compounds with the K^+ ions outside the brackets, even though they coordinate directly with the POMs. Other Ln-containing complexes are isostructural with the gadolinium analogues.

2. Results and Discussion

2.1. Synthesis

Several approaches were described in the literature for the preparation of Ln-POM complexes differing in the lacunary phosphotungstate precursors, such as $[PW_9O_{34}]^{9-}$ [43] or $[P_2W_{19}O_{69}(H_2O)]^{14-}$ [50]. In our work, we used a monolacunary $[PW_{11}O_{39}]^{7-}$ polyoxoanion to react with Ln cations, and the pH value was set at 5.4. As a result, we obtained crystals of three different kinds simultaneously. We were succeeded in structurally characterizing all three types of crystals for the gadolinium-containing compounds, and the unit cell parameters for the three types were also determined in the case of europium. For praseodymium, it was possible to determine the parameters of two types of crystals, and only one type was characterized in the case of dysprosium and terbium (Table 1). The resulting phases were additionally characterized by IR spectroscopy (Figure S1).

Table 1. Unit cell parameters for selected crystals of the compounds: V (Å^3), a (Å), b (Å), c (Å), α (°), β (°), and γ (°).

Ln	**1, *P*–1**		**2, *P*–1**		**3, $P2_1/c$**	
Pr	2498	11.82 12.28 19.62 94.6 91.0 118.1			6053	13.11 22.08 21.35 90 101.7 90
Eu	2386	11.8 11.9 19.4 96.0 92.1 117.7	3305	12.81 13.04 23.41 73.1 83.9 62.1	5856	13.0 22.1 20.7 90 100.0 90
Gd	2380	11.73 11.92 19.39 95.85 92.30 117.57	3289	12.8 13.0 23.3 73.8 84.3 61.8	5799	12.96 22.10 20.68 90 100.11 90
Tb	2407	11.75 11.97 19.53 96.1 92.1 117.7				
Dy			3267	12.72 13.04 23.20 74.0 81.3 62.1		

2.2. Structural Description

The structure of $(Me_4N)_2K_2[Gd(H_2O)_2PW_{11}O_{39}]\cdot5H_2O$ (**1Gd**) is presented in Figure 1a,b. The Gd is incorporated to the vacant site of the $\{PW_{11}O_{39}\}$ POM, coordinating via four O atoms (Figure 1a). The Gd further coordinates two neighboring POMs, thus forming a chain with the $\{Gd_2(POM)_2\}$ secondary building unit (Figure 1b), similarly to that in works [43,64]. The coordination sphere of Gd is supplemented by two H_2O ligands, resulting in a $\{GdO_8\}$ polyhedron with the typical Gd–O distances. Potassium counterions join the chains into layers via K–O bonds with the POMs (Figure 2a,b). Me_4N^+, and disordered hydrate molecules are located between the layers.

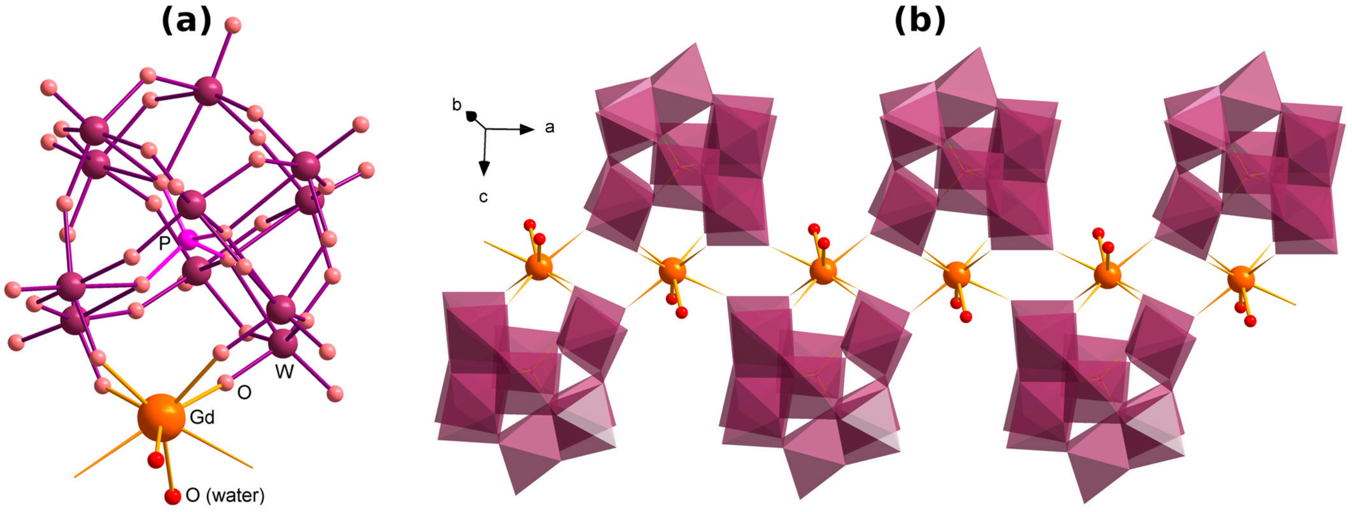

Figure 1. (**a**) The structure of $\{Gd(H_2O)_2PW_{11}O_{39}\}$ unit in compound **1Gd**; (**b**) the corresponding $\{Gd(H_2O)_2PW_{11}O_{39}\}_n$ chain. The WO_6 moieties are depicted as octahedra.

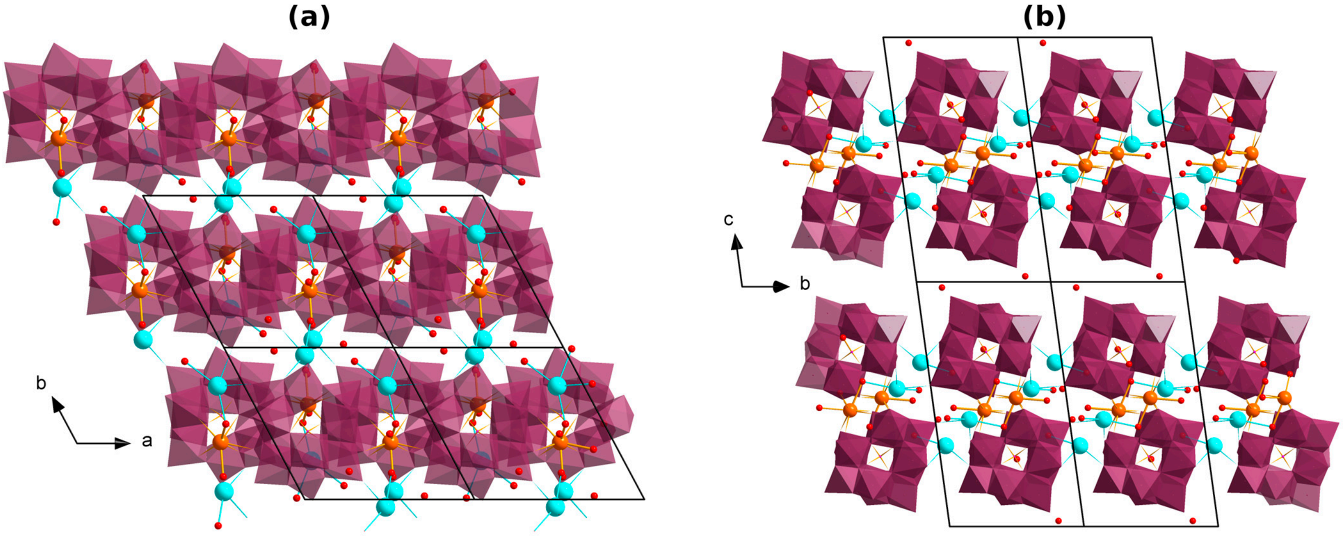

Figure 2. (**a**) The structure of a layer composed from $\{Gd(H_2O)_2PW_{11}O_{39}\}_n$ chains bound with K^+ cations in compound **1Gd**; (**b**) the crystal packing of the layers. Me_4N^+ and hydrogens are not shown, the WO_6 moieties are depicted as octahedra.

The structure of **2Gd** and **3Gd** somewhat resembles **1Gd** in that they comprise a $\{Gd_2(POM)_2\}$ secondary building unit. However, in **2Gd** and **3Gd**, it is not interlocked in a chain but is supplemented by two terminating H_2O ligands, thus forming a centrosymmetric dimer structure (Figure 3). Analogous dimeric structures with different counterions ($Na^+/H^+/Me_4N^+$) have recently been reported [34,50]. The coordination polyhedron $\{GdO_8\}$ is similar in the compounds. Contrary to **1Gd**, the structures of **2Gd** and **3Gd** reveal a disorder of K^+ and Me_4N^+, i.e., the latter take partial occupancy, sharing similar positions with the hydrate molecules. The ratio of the cations is approximately similar within the series (tested for several crystals of **2** or **3**). Due to the complicated disorder, positions of the counterions and the hydrate molecules are rather arbitrary. We speculate that the disordered K^+ can both coordinate directly with the POM and bind via a hydrogen bond network. The number of the outer-sphere H_2O and Me_4N^+ in **2Gd** and **3Gd** is larger than in **1Gd**, so the POM species are more separated from each other in the former. The difference between **2Gd** and **3Gd** consists in different crystal packing of the POMs, which is induced by a variation in the outer-sphere composition (Figure 4). Specifically, in **2Gd**, the POMs are located one above the other with the translation relation (P–1 space group), while in **3Gd**, neighboring POMs are oriented by an angle of ca. 40° with respect to each other (relation by two-fold screw symmetry; $P2_1/c$ space group).

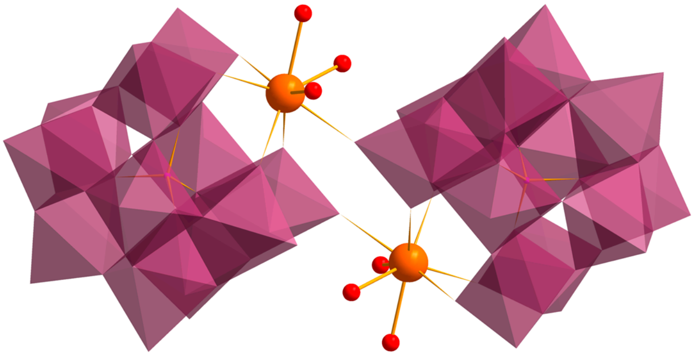

Figure 3. The structure of a dimer $\{Gd(H_2O)_3PW_{11}O_{39}\}_2$ in compounds **2Gd** and **3Gd**.

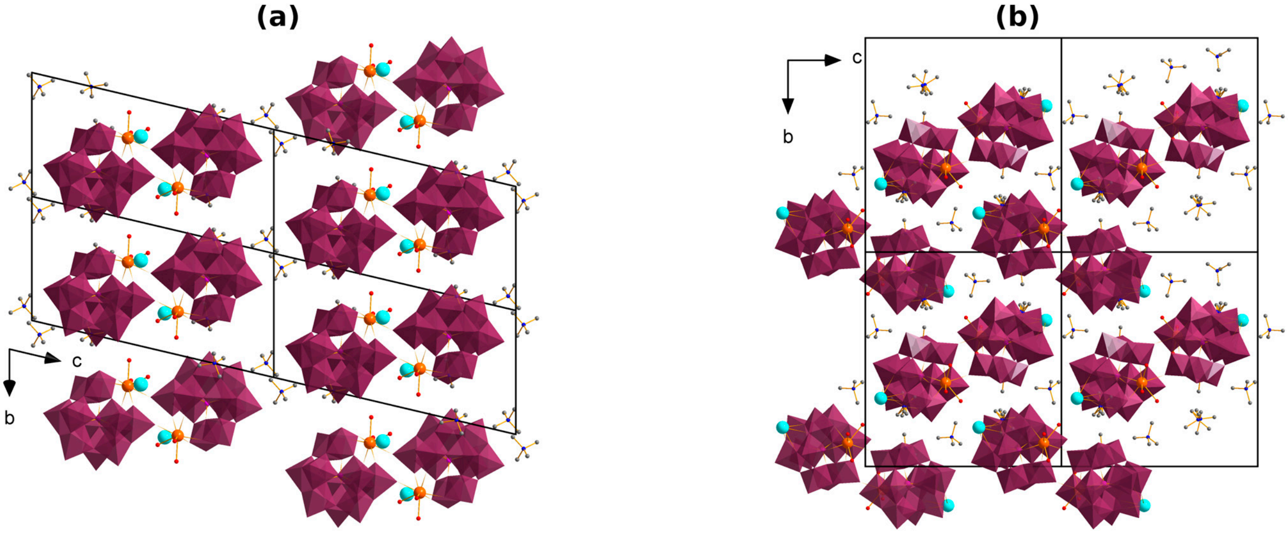

Figure 4. Crystal packing of the dimers in compounds **2Gd** (**a**) and **3Gd** (**b**). The WO_6 moieties are depicted as octahedra, hydrate molecules, hydrogens and the disorder are not shown.

Other lanthanide analogues with Pr, Eu, Tb and Dy also constitute three structural types **1–3**, which are identified by unit cell parameters of single crystals (Table 1). One can note that the unit cell parameters generally correlate with the ionic radius of the lanthanides. At the same time, experiments within one lanthanide series reveal a quite large variation of the parameters above the instrument accuracy. Specifically, the unit cell volume for several crystals of **3Pr** varies by 100 Å^3, while the difference in parameter c can be up to 0.46 Å (Table 2). This is likely a consequence of the non-stoichiometric composition of disordered hydrate molecules in the compounds, which varies from crystal to crystal.

Table 2. Unit cell parameters for several crystals of **3Pr** ($P2_1/c$ space group): V (Å^3), a (Å), b (Å), c (Å), and β (°).

	V	*a*	*b*	*c*	β
crystal 1	5969.5 (9)	13.0360 (8)	21.9985 (11)	21.228 (2)	101.300 (9)
crystal 2	5889.3 (9)	13.0069 (10)	22.0055 (16)	20.908 (3)	100.228 (9)
crystal 3	5878.9 (6)	13.0061 (7)	22.0170 (14)	20.858 (2)	100.174 (6)
crystal 4	5851.2 (5)	13.0038 (10)	21.9926 (12)	20.7695 (12)	99.905 (5)

3. Experimental Section

3.1. Materials and Methods

The $K_7[PW_{11}O_{39}]\cdot 14H_2O$ precursor was prepared according to the literature [66] and confirmed by IR spectra. Other chemicals were purchased commercially from Sigma Aldrich and used without further purification. Infrared spectra (4000–400 cm^{-1}) were recorded on a Scimitar FTS 2000 spectrophotometer in KBr pressed pellets.

3.2. Synthesis

Synthesis of $Cat_4Gd(PW_{11}O_{39})\cdot xH_2O$: First, 1.00 g (0.31 mmol) of $K_7[PW_{11}O_{39}]\cdot 14H_2O$ was dissolved in 15 mL of water, which was followed by the addition of 0.20 g (0.54 mmol) of $GdCl_3\cdot 6H_2O$ in 15 mL of water dropwise, resulting in a pH = 4.7. The pH value was adjusted to 5.4 using 2M KOH solution under stirring. The reaction mixture was heated at 80 °C for 1 h after the solution was cooled to room temperature and filtered. Then, 0.20 g (1.30 mmol) of tetramethylammonium bromide was added under stirring. After 0.5 h, the resulting solution was filtered and left to evaporate at room temperature. A crystalline phase was obtained after one week. Yield: ca. 43% (based on $K_7[PW_{11}O_{39}]\cdot 14H_2O$).

Synthesis of $Cat_4Pr(PW_{11}O_{39})·xH_2O$: The synthetic procedure was identical to that for Gd-POMs, but we used 0.2 g (0.54 mmol) of $PrCl_3·7H_2O$ as the Ln reagent. A crystalline phase was obtained after one week. Yield: ca. 35% (based on $K_7[PW_{11}O_{39}]·14H_2O$).

Synthesis of $Cat_4Eu(PW_{11}O_{39})·xH_2O$: The synthetic procedure was identical to that for Gd-POMs, but we used 0.2 g (0.55 mmol) of $EuCl_3·6H_2O$ as the Ln reagent. A crystalline phase was obtained after one week. Yield: ca. 51% (based on $K_7[PW_{11}O_{39}]·14H_2O$).

Synthesis of $Cat_4Tb(PW_{11}O_{39})·xH_2O$: The synthetic procedure was identical to that for Gd-POMs, but we used 0.2 g (0.54 mmol) of $TbCl_3·6H_2O$ as the Ln reagent. A crystalline phase was obtained after one week. Yield: ca. 24% (based on $K_7[PW_{11}O_{39}]·14H_2O$).

Synthesis of $Cat_4Dy(PW_{11}O_{39})·xH_2O$: The synthetic procedure was identical to that for Gd-POMs, but we used 0.2 g (0.53 mmol) of $DyCl_3·6H_2O$ as the Ln reagent. A crystalline phase was obtained after one week. Yield: ca. 27% (based on $K_7[PW_{11}O_{39}]·14H_2O$).

3.3. X-Ray Diffraction on Single Crystals

Single-crystal XRD data for the compounds were collected at 150 K (Table S1) with a Bruker D8 Venture diffractometer with a CMOS PHOTON III detector (Bruker, Madison, Wisconsin, USA) and IμS 3.0 microfocus source (MoK_α radiation (λ = 0.71073 Å), collimating Montel mirrors; Incoatec GmbH, Geesthacht, Germany). The crystal structures were solved using the SHELXT [67] and were refined using the SHELXL [68] programs with OLEX2 GUI [69]. Atomic displacement parameters for non-hydrogen atoms were refined in anisotropic approximation with the exception for the disordered hydrate molecules and Me_4N^+. For the latter, EADP constraints and SADI restraints were applied where needed. Hydrogen atoms were placed geometrically and refined in the riding model with the exception for those of the disordered hydrate molecules, which were not localized. The structures of **1–3Gd** were deposited to the Cambridge Crystallographic Data Centre (CCDC) as a supplementary publication, No. 2270528-2270530.

4. Conclusions

A series of 1:1 Ln^{3+}/POM (Ln = Pr, Eu, Gd, Tb, Dy) complexes of the general formula $Cat_4Ln(PW_{11}O_{39})·xH_2O$ (Cat = K^+ or Me_4N^+) was synthesized in an aqueous solution. It was shown that the $\{Ln(PW_{11}O_{39})\}$ fragments are always involved in binding with each other to form either polymer chains or dimeric units, and the Ln^{3+} coordination number is the same in all cases and equals 8. It was also found that for the isostructural compounds, the unit cell parameters mainly correlate with the corresponding ionic radius of the lanthanides. The description of these compounds is important for the study of other monovacant POMs of the Keggin type in an aqueous solution and should be taken into account when developing {Ln-POM} hybrid complexes.

Supplementary Materials: The supporting information can be downloaded at: https://www.mdpi.com/article/10.3390/inorganics11080327/s1, Figure S1: IR spectra of $Cat_4Ln(PW_{11}O_{39})·xH_2O$ complexes (Ln from the top to the bottom): Gd, Eu, Pr, Tb and Dy; Table S1. Crystal data and structure refinement for **1–3Gd**.

Author Contributions: Conceptualization, M.N.S.; methodology, V.S.K. and M.N.S.; analysis, V.S.K. and T.S.S.; investigation, V.S.K. and T.S.S.; writing—original draft preparation, V.S.K. and T.S.S.; writing—review and editing, V.S.K. and M.N.S.; visualization, V.S.K. and T.S.S. All authors have read and agreed to the published version of the manuscript.

Funding: This work was supported by the Ministry of Science and Higher Education of the Russian Federation, № 121031700313-8 (The Nikolaev Institute of Inorganic Chemistry SB RAS).

Data Availability Statement: The data presented in this study are available on request from the corresponding author.

Acknowledgments: The authors thank the NIIC SB RAS team for the access to IR and SCXRD facilities.

Conflicts of Interest: The authors declare no conflict of interest.

References

1. Pope, M.T. *Heteropoly and Isopoly Oxometalates*; Springer: Berlin/Heidelberg, Germany, 1983.
2. Pope, M.T.; Müller, A. *Polyoxometalates: From Platonic Solids to Anti-Retroviral Activity*; Kluwer Academic Publishers: Dordrecht, The Netherlands, 1994. [CrossRef]
3. Yamase, T.; Pope, M.T. *Polyoxometalates Chemistry for Nano-Composite Design*; Kluwer Academic/Plenum Publishers: New York, NY, USA, 2002. [CrossRef]
4. Lehmann, J.; Gaita-Arino, A.; Coronado, E.; Loss, D. Quantum computing with molecular spin systems. *J. Mater. Chem.* **2009**, *19*, 1672–1677. [CrossRef]
5. Charron, G.; Giusti, A.; Mazerat, S.; Mialane, P.; Gloter, A.; Miserque, F.; Keita, B.; Nadjo, L.; Filoramo, A.; Rivière, E.; et al. Assembly of a magnetic polyoxometalate on SWNTs. *Nanoscale* **2010**, *2*, 139–144. [CrossRef] [PubMed]
6. Newton, G.N.; Yamashita, S.; Hasumi, K.; Matsuno, J.; Yoshida, N.; Nihei, M.; Shiga, T.; Nakano, M.; Nojiri, H.; Wernsdorfer, W.; et al. Redox-Controlled Magnetic {Mn_{13}} Keggin Systems. *Angew. Chem. Int. Ed.* **2011**, *50*, 5715–5720. [CrossRef]
7. AlDamen, M.A.; Cardona-Serra, S.; Clemente-Juan, J.; Coronado, E.; Gaita-Arino, A.; Marti-Gastaldo, C.; Luis, F.; Montero, O. Mononuclear Lanthanide Single Molecule Magnets Based on the Polyoxometalates $[Ln(W_5O_{18})_2]^{9-}$ and $[Ln(\beta_2\text{-}SiW_{11}O_{39})_2]^{13-}$ (Ln^{III} = Tb, Dy, Ho, Er, Tm, and Yb). *Inorg. Chem.* **2009**, *48*, 3467–3479. [CrossRef]
8. Ritchie, C.; Ferguson, A.; Nojiri, H.; Miras, H.N.; Song, Y.-F.; Long, D.-L.; Burkholder, E.; Murrie, M.; Kögerler, P.; Brechin, E.K.; et al. Polyoxometalate-Mediated Self-Assembly of Single-Molecule Magnets: $\{[XW_9O_{34}]_2[Mn^{III}{}_4Mn^{II}{}_2O_4(H_2O)_4]\}^{12-}$. *Angew. Chem. Int. Ed.* **2008**, *47*, 5609–5612. [CrossRef]
9. AlDamen, M.A.; Clemente-Juan, J.M.; Coronado, E.; Marti-Gastaldo, C.; Gaita-Ariño, A. Mononuclear Lanthanide Single-Molecule Magnets Based on Polyoxometalates. *J. Am. Chem. Soc.* **2008**, *130*, 8874–8875. [CrossRef]
10. Compain, J.D.; Mialane, P.; Dolbecq, A.; Mbomekallé, I.M.; Marrot, J.; Sécheresse, F.; Rivière, E.; Rogez, G.; Wernsdorfer, W. Iron Polyoxometalate Single-Molecule Magnets. *Angew. Chem. Int. Ed.* **2009**, *48*, 3077–3081. [CrossRef]
11. Weiner, H.; Finke, R.G. An All-Inorganic, Polyoxometalate-Based Catechol Dioxygenase That Exhibits >100 000 Catalytic Turnovers. *J. Am. Chem. Soc.* **1999**, *121*, 9831–9842. [CrossRef]
12. Maksimchuk, N.V.; Timofeeva, M.N.; Melgunov, M.S.; Shmakov, A.N.; Chesalov, Y.A.; Dybtsev, D.N.; Fedin, V.P.; Kholdeeva, O.A. Heterogeneous selective oxidation catalysts based on coordination polymer MIL-101 and transition metal-substituted polyoxometalates. *J. Catal.* **2008**, *257*, 315–323. [CrossRef]
13. Kikukawa, Y.; Yamaguchi, K.; Mizuno, N. Zinc(II) Containing γ-Keggin Sandwich-Type Silicotungstate: Synthesis in Organic Media and Oxidation Catalysis. *Angew. Chem. Int. Ed.* **2010**, *49*, 6096–6100. [CrossRef]
14. Okuhara, T.; Mizuno, N.; Misono, M. Catalysis by heteropoly compounds—Recent developments. *Appl. Catal. A* **2001**, *222*, 63–77. [CrossRef]
15. Zhang, T.R.; Liu, S.Q.; Kurth, D.G.; Faul, C.F.J. Organized Nanostructured Complexes of Polyoxometalates and Surfactants that Exhibit Photoluminescence and Electrochromism. *Adv. Funct. Mater.* **2009**, *19*, 642–652. [CrossRef]
16. Cooper, G.J.T.; Cronin, L. Real-Time Direction Control of Self Fabricating Polyoxometalate-Based Microtubes. *J. Am. Chem. Soc.* **2009**, *131*, 8368–8369. [CrossRef] [PubMed]
17. Kawasaki, N.; Wang, H.; Nakanishi, R.; Hamanaka, S.; Kitaura, R.; Shinohara, H.; Yokoyama, T.; Yoshikawa, H.; Awaga, K. Nanohybridization of Polyoxometalate Clusters and Single-Wall Carbon Nanotubes: Applications in Molecular Cluster Batteries. *Angew. Chem. Int. Ed.* **2011**, *50*, 3471–3474. [CrossRef] [PubMed]
18. Geisberger, G.; Paulus, S.; Carraro, M.; Bonchio, M.; Patzke, G.R. Synthesis, Characterisation and Cytotoxicity of Polyoxometalate/Carboxymethyl Chitosan Nanocomposites. *Chem.–Eur. J.* **2011**, *17*, 4619–4625. [CrossRef]
19. Wall, M.J.; Wigmore, G.; Lopatar, J.; Frenguelli, B.G.; Dale, N. The novel NTPDase inhibitor sodium polyoxotungstate (POM-1) inhibits ATP breakdown but also blocks central synaptic transmission, an action independent of NTPDase inhibition. *Neuropharmacology* **2008**, *55*, 1251–1258. [CrossRef]
20. Musumeci, C.; Luzio, A.; Pradeep, C.P.; Miras, H.N.; Rosnes, M.H.; Song, Y.F.; Long, D.L.; Cronin, L.; Pignataro, B. Programmable Surface Architectures Derived from Hybrid Polyoxometalate-Based Clusters. *J. Phys. Chem. C* **2011**, *115*, 4446–4455. [CrossRef]
21. Grzhegorzhevskii, K.V.; Shevtsev, N.S.; Abushaeva, A.R.; Chezganov, D.S.; Ostroushko, A.A. Prerequisites and prospects for the development of novel systems based on the Keplerate type polyoxomolybdates for the controlled release of drugs and fluorescent molecules. *Russ. Chem. Bull.* **2020**, *69*, 804–814. [CrossRef]
22. Cavaleiro, A.M.V.; Pedrosa de Jesus, J.D.; Noguera, H.I.S. *Metal Clusters in Chemistry*; Wiley-VCH: London, UK, 1999. [CrossRef]
23. Yamase, T. Photo- and Electrochromism of Polyoxometalates and Related Materials. *Chem. Rev.* **1998**, *98*, 307–326. [CrossRef]
24. Sadakane, M.; Dickman, M.H.; Pope, M.T. Controlled Assembly of Polyoxometalate Chains from Lacunary Building Blocks and Lanthanide-Cation Linkers. *Angew. Chem. Int. Ed.* **2000**, *39*, 2914–2916. [CrossRef]
25. Mialane, P.; Lisnard, L.; Mallard, A.; Marrot, J.; Antic-Fidancev, E.; Aschehoug, P.; Vivien, D.; Secheresse, F. Solid-State and Solution Studies of {$Ln_n(SiW_{11}O_{39})$} Polyoxoanions: An Example of Building Block Condensation Dependent on the Nature of the Rare Earth. *Inorg. Chem.* **2003**, *42*, 2102–2108. [CrossRef] [PubMed]
26. Muller, A.; Peters, F.; Pope, M.T.; Gatteschi, D. Polyoxometalates: Very Large Clusters—Nanoscale Magnets. *Chem. Rev.* **1998**, *98*, 239–271. [CrossRef] [PubMed]
27. Wassermann, K.; Dickman, M.H.; Pope, M.T. Self-Assembly of Supramolecular Polyoxometalates: The Compact, Water-Soluble Heteropolytungstate Anion $[As^{III}{}_{12}Ce^{III}{}_{16}(H_2O)_{36}W_{148}O_{524}]^{76-}$. *Angew. Chem. Int. Ed. Engl.* **1997**, *36*, 1445–1448. [CrossRef]

28. Belai, N.; Sadakane, M.; Pope, M.T. Formation of Unsymmetrical Polyoxotungstates via Transfer of Polyoxometalate Building Blocks. NMR Evidence Supports the Kinetic Stability of the Pentatungstate Anion, $[W_5O_{18}]^{6-}$, in Aqueous Solution. *J. Am. Chem. Soc.* **2001**, *123*, 2087–2088. [CrossRef] [PubMed]
29. Wu, H.; Zhi, M.; Chen, H.; Singh, V.; Ma, P.; Wang, J.; Niu, J. Well-tuned white-light-emitting behaviours in multicenter-Ln polyoxometalate derivatives: A photoluminescence property and energy transfer pathway study. *Spectrochim. Acta—A Mol. Biomol. Spectrosc.* **2019**, *223*, 117294. [CrossRef]
30. Wang, K.; Feng, S.; Ma, P. Synthesis, characterization and photoluminescence properties of a benzoic modified lanthanide-containing polyoxometalate. *Inorg. Chem. Commun.* **2019**, *108*, 107511. [CrossRef]
31. Wu, H.; Yan, B.; Liang, R.; Singh, V.; Ma, P.; Wang, J.; Niu, J. An organic chromophore—Modified samarium-containing polyoxometalate: Excitation-dependent color tunable behavior from the organic chromophores to the lanthanide ion. *Dalton Trans.* **2020**, *49*, 388–394. [CrossRef]
32. Wang, K.; Feng, S.; Ma, P. Synthesis, characterization and photoluminescence properties of an organic–inorganic hybrid monolacunary Keggin-type polyoxotungstate. *Inorg. Chem. Commun.* **2021**, *129*, 108621. [CrossRef]
33. Sarwar, S.; Sanz, S.; van Leusen, J.; Nichol, G.S.; Brechin, E.K.; Kögerler, P. Phthalocyanine-polyoxotungstate lanthanide double deckers. *Dalton Trans.* **2020**, *49*, 16638–16642. [CrossRef]
34. Niu, J.; Wang, K.; Chen, H.; Zhao, J.; Ma, P.; Wang, J.; Li, M.; Bai, Y.; Dang, D. Assembly Chemistry between Lanthanide Cations and Monovacant Keggin Polyoxotungstates: Two Types of Lanthanide Substituted Phosphotungstates $[\{(\alpha\text{-}PW_{11}O_{39}H)Ln(H_2O)_3\}_2]^{6-}$ and $[\{(\alpha\text{-}PW_{11}O_{39})Ln(H_2O)(\eta^2,\mu\text{-}1,1)\text{-}CH_3COO\}_2]^{10-}$. *Cryst. Growth Des.* **2009**, *9*, 4362–4372. [CrossRef]
35. Zhang, D.; Zhang, C.; Chen, H.; Ma, P.; Wang, J.; Niu, J. Syntheses, structures and properties of dimeric rare earth derivatives based on monovacant Keggin-type polyoxotungstates. *Inorg. Chim. Acta* **2012**, *391*, 218–223. [CrossRef]
36. Zhao, H.-Y.; Zhao, J.-W.; Yang, B.-F.; He, H.; Yang, G.-Y. Organic–inorganic hybrids based on monovacant Keggin-type polyoxotungstates and 3d–4f heterometals. *CrystEngComm* **2013**, *15*, 8186–8194. [CrossRef]
37. Zhao, H.-Y.; Zhao, J.-W.; Yang, B.-F.; Wei, Q.; Yang, G.-Y. Two Organic–Inorganic Hybrids Assembled by Carboxylate-Bridging Lanthanide-Substituted Polyoxometalate Dimers with Copper–ethylendiamine Cations. *J. Clust. Sci.* **2014**, *25*, 667–680. [CrossRef]
38. Zhang, S.; Wang, Y.; Zhao, J.; Ma, P.; Wang, J.; Niu, J. Two types of oxalate-bridging rare-earth-substituted Keggin-type phosphotungstates $\{[(\alpha\text{-}PW_{11}O_{39})RE(H_2O)]_2(C_2O_4)\}^{10-}$ and $\{(\alpha\text{-}x\text{-}PW_{10}O_{38})RE_2(C_2O_4)(H_2O)_2\}^{3-}$. *Dalton Trans.* **2012**, *41*, 3764–3772. [CrossRef] [PubMed]
39. Ma, P.; Hu, F.; Wan, R.; Huo, Y.; Zhang, D.; Niu, J.; Wang, J. Magnetic double-tartaric bridging mono-lanthanide substituted phosphotungstates with photochromic and switchable luminescence properties. *J. Mater. Chem. C* **2016**, *4*, 5424–5433. [CrossRef]
40. Wu, H.; Zhi, M.; Singh, V.; Li, H.; Ma, P.; Niu, J.; Wang, J. Elucidating white light emissions in Tm^{3+}/Dy^{3+} codoped polyoxometalates: A color tuning and energy transfer mechanism study. *Dalton Trans.* **2018**, *47*, 13949–13956. [CrossRef]
41. Wang, K.; Zhang, D.; Ma, J.; Ma, P.; Niu, J.; Wang, J. Three-dimensional lanthanide polyoxometalate organic complexes: Correlation of structure with properties. *CrystEngComm* **2012**, *14*, 3205–3212. [CrossRef]
42. Peacock, R.D.; Weakley, T.J.R. Heteropolytungstate complexes of the lanthanide elements. Part I. Preparation and reactions. *J. Chem. Soc. A* **1971**, 1836–1839. [CrossRef]
43. Zhang, C.; Howell, R.C.; Scotland, K.B.; Perez, F.G.; Todaro, L.; Francesconi, L.C. Aqueous Speciation Studies of Europium(III) Phosphotungstate. *Inorg. Chem.* **2004**, *43*, 7691–7701. [CrossRef]
44. Fan, L.; Xu, L.; Gao, G.; Li, F.; Li, Z.; Qiu, Y. A novel polyoxometalate chain constructed from sandwich lanthanide-containing polyanion $[Ce(PW_{11}O_{39})_2]^{10-}$ and sodium ion linker. *Inorg. Chem. Commun.* **2006**, *9*, 1308–1311. [CrossRef]
45. Fan, L.-H.; Xu, L.; Zhang, C.-H.; Li, F.-Y.; Li, Z.-K.; Liu, X.-Z. A novel polyoxometalate chain constructed from sandwich lanthanide-containing polyanions $[Pr(PW_{11}O_{39})_2]^{11-}$ and sodium cation linkers. *Struct. Chem.* **2007**, *18*, 917–921. [CrossRef]
46. Iijima, J.; Ishikawa, E.; Nakamura, Y.; Naruke, H. Synthesis and structural investigation of sandwich polyoxotungstates containing cerium (III/IV) and mono-lacunary Keggin tungstophosphate units. *Inorg. Chim. Acta* **2010**, *363*, 1500–1506. [CrossRef]
47. Iijima, J.; Naruke, H. Structural characterization of Keggin sandwich-type $[Ln^{III}(\alpha\text{-}PW_{11}O_{39})_2]^{11-}$ (Ln = La and Ce) anion containing a pseudo-cubic $Ln^{III}O_8$ center. *Inorg. Chim. Acta* **2011**, *379*, 95–99. [CrossRef]
48. Gupta, R.; Saini, M.K.; Doungmene, F.; de Oliveira, P.; Hussain, F. Lanthanoid containing phosphotungstates: The syntheses, crystal structure, electrochemistry, photoluminescence and magnetic properties. *Dalton Trans.* **2014**, *43*, 8290–8299. [CrossRef] [PubMed]
49. Wen, H.-R.; Lu, X.-N.; Liao, J.-S.; Zhang, C.-W.; You, H.-Y.; Liu, C.-M. Preparation and luminescence properties of phosphors of rare earth complexes based on polyoxotungstates. *Mater. Res. Bull.* **2015**, *68*, 16–21. [CrossRef]
50. Ma, P.; Hu, F.; Huo, Y.; Zhang, D.; Zhang, C.; Niu, J.; Wang, J. Magnetoluminescent Bifunctional Dysprosium-Based Phosphotungstates with Synthesis and Correlations between Structures and Properties. *Cryst. Growth Des.* **2017**, *17*, 1947–1956. [CrossRef]
51. Li, Z.; Lin, L.-D.; Zhao, D.; Sun, Y.-Q.; Zheng, S.-T. A Series of Unprecedented Linear Mixed-Metal-Substituted Polyoxometalate Trimers: Syntheses, Structures, Luminescence, and Proton Conductivity Properties. *Eur. J. Inorg. Chem.* **2019**, *3–4*, 437–441. [CrossRef]
52. Naruke, H.; Iijima, J.; Sanji, T. Enantioselective Resolutions and Circular Dichroism Studies of Lanthanide-Containing Keggin-Type $[Ln(PW_{11}O_{39})_2]^{11-}$ Polyoxometalates. *Inorg. Chem.* **2011**, *50*, 7535–7539. [CrossRef]

53. Liu, Y.; Li, H.; Zhang, J.; Zhao, J.; Chen, L. Synthesis, structure, spectroscopic and ferroelectric properties of an acentric polyoxotungstate containing 1:2-type $[Sm(\alpha\text{-}PW_{11}O_{39})_2]^{11-}$ fragment and d-proline components. *Spectrochim. Acta—A Mol. Biomol. Spectrosc.* **2015**, *134*, 101–108. [CrossRef]
54. Iijima, J.; Naruke, H.; Sanji, T. On chirality induction in the crystalline solid-containing sandwich-type $[Ln(\alpha\text{-}PW_{11}O_{39})_2]^{11-}$ polyoxotungstate and proline. *RSC Adv.* **2016**, *6*, 91494–91507. [CrossRef]
55. Liu, Y.-H.; Guo, G.-L.; Wang, J.-P. Hydrothermal synthesis and crystal structure of a heteropolyoxotungstate formed by sandwich-type heteropolyanion $[Gd(PW_{11}O_{39})_2]^{11-}$ and reduced $[Cu(en)_2]^+$ cations. *J. Coord. Chem.* **2008**, *61*, 2428–2436. [CrossRef]
56. Du, D.-Y.; Qin, J.-S.; Li, S.-L.; Wang, X.-L.; Yang, G.-S.; Li, Y.-G.; Shao, K.-Z.; Su, Z.-M. A series of inorganic–organic hybrid compounds constructed from bis(undecatungstophosphate) lanthanates and copper-organic units. *Inorg. Chim. Acta* **2010**, *363*, 3823–3831. [CrossRef]
57. Du, D.-Y.; Qin, J.-S.; Yuan, G.; Lan, Y.-Q.; Wang, X.-L.; Shao, K.-Z.; Su, Z.-M. Building block approach to a series of substituted Keggin-type inorganic–organic hybrids. *Solid State Sci.* **2011**, *13*, 1115–1121. [CrossRef]
58. Chen, L.; Shi, D.; Wang, Y.; Cheng, H.; Geng, Z.; Zhao, J.; Ma, P.; Niu, J. Two 3d–4f heterometallic monovacant Keggin phosphotungstate derivatives. *J. Coord. Chem.* **2011**, *64*, 400–412. [CrossRef]
59. Shi, D.; Chen, L.; Zhao, J.; Wang, Y.; Ma, P.; Niu, J. Two novel 2D organic–inorganic hybrid lacunary Keggin phosphotungstate 3d–4f heterometallic derivatives: $[Cu(en)_2]_2H_6[Ce(\alpha\text{-}PW_{11}O_{39})_2]\cdot 8H_2O$ and $[Cu(dap)_2(H_2O)][Cu(dap)_2]_{4.5}[Dy(\alpha\text{-}PW_{11}O_{39})_2]\cdot 4H_2O$. *Inorg. Chem. Commun.* **2011**, *14*, 324–329. [CrossRef]
60. Shi, D.; Wang, Z.; Xing, J.; Li, Y.; Luo, J.; Chen, L.; Zhao, J. A 2-D Organic–Inorganic Hybrid Copper-Yttrium Heterometallic Monovacant Keggin Phosphotungstate Derivative: $[Cu(dap)_2]_{5.5}[Y(\alpha\text{-}PW_{11}O_{39})_2]\cdot 4H_2O$. *Synth. React. Inorg. Metalorg. Nanometal. Chem.* **2012**, *42*, 30–36. [CrossRef]
61. Li, Y.; Tian, S.; Li, Y.-Z.; Zhao, J.; Ma, P.; Chen, L. Two 2D Cu–Ln heterometallic polyoxometalate aggregates constructed from bis(undecatungstophosphate)lanthanate units and copper-complex bridges. *Inorg. Chim. Acta* **2013**, *405*, 105–110. [CrossRef]
62. Zhang, J.; Yan, X.; Shi, D.; Zhao, J.; Chen, L. Synthesis, Structure, and Properties of a 2-D Organic–Inorganic Hybrid Phosphotungstate-Based Cu^{II}–La^{III} Heterometallic Derivative. *Synth. React. Inorg. Metalorg. Nanometal. Chem.* **2014**, *44*, 171–176. [CrossRef]
63. Zhao, H.-Y.; Yang, B.-F.; Yang, G.-Y. Two new 2D organic–inorganic hybrids assembled by lanthanide-substituted polyoxotungstate dimers and copper–complex linkers. *Inorg. Chem. Commun.* **2017**, *84*, 212–216. [CrossRef]
64. Zhang, C.; Ma, P.; Chen, H.; Wang, J.; Niu, J. Synthesis, structure, and properties of a 1-D cerium based on monovacant Keggin-type polyoxotungstate. *J. Coord. Chem.* **2011**, *64*, 2178–2185. [CrossRef]
65. Ma, P.; Si, Y.; Wan, R.; Zhang, S.; Wang, J.; Niu, J. Synthesis, crystal structure, and properties of a 1-D terbium-substituted monolacunary Keggin-type polyoxotungstate . *Spectrochim. Acta—A Mol. Biomol. Spectrosc.* **2015**, *138*, 579–584. [CrossRef] [PubMed]
66. Contant, R. Relations entre les tungstophosphates apparentés à l'anion $PW_{12}O_{40}{}^{3-}$. Synthèse et propriétés d'un nouveau polyoxotungstophosphate lacunaire $K_{10}P_2W_{20}O_{70}\cdot 24H_2O$. *Can. J. Chem.* **1987**, *65*, 568–573. [CrossRef]
67. Sheldrick, G. SHELXT—Integrated space-group and crystal-structure determination. *Acta Crystallogr. Sect. A* **2015**, *71*, 3–8. [CrossRef] [PubMed]
68. Sheldrick, G.M. Crystal structure refinement with SHELXL. *Acta Crystallogr. Sect. C* **2015**, *71*, 3–8. [CrossRef] [PubMed]
69. Dolomanov, O.V.; Bourhis, L.J.; Gildea, R.J.; Howard, J.A.K.; Puschmann, H. OLEX2: A complete structure solution, refinement and analysis program. *J. Appl. Crystallogr.* **2009**, *42*, 339–341. [CrossRef]